Geophysical Research Letters

RESEARCH LETTER
10.1029/2023GL105265

Differences Between the CMIP5 and CMIP6 Antarctic Sea Ice Concentration Budgets

Yafei Nie[1], Xia Lin[2,3], Qinghua Yang[1], Jiping Liu[1], Dake Chen[1], and Petteri Uotila[4]

[1]School of Atmospheric Sciences, Sun Yat-Sen University, and Southern Marine Science and Engineering Guangdong Laboratory (Zhuhai), Zhuhai, China, [2]School of Marine Sciences, Nanjing University of Information Science and Technology, Nanjing, China, [3]Earth and Life Institute, Université Catholique de Louvain, Louvain-la-Neuve, Belgium, [4]Institute for Atmospheric and Earth System Research/ Physics, Faculty of Science, University of Helsinki, Helsinki, Finland

Key Points:

- The Antarctic sea ice concentration (SIC) budgets in CMIP6 have improved from CMIP5
- The ice-ocean coupled models have more realistic SIC budgets than fully coupled models, except for the excessive velocity convergence
- Underestimation of velocity divergence in the model was found to be strongly associated with underestimation of sea ice thickness

Supporting Information:

Supporting Information may be found in the online version of this article.

Correspondence to:

Q. Yang,
yangqh25@mail.sysu.edu.cn

Citation:

Nie, Y., Lin, X., Yang, Q., Liu, J., Chen, D., & Uotila, P. (2023). Differences between the CMIP5 and CMIP6 Antarctic sea ice concentration budgets. *Geophysical Research Letters*, *50*, e2023GL105265. https://doi.org/10.1029/2023GL105265

Received 29 JUN 2023
Accepted 16 NOV 2023

Author Contributions:

Conceptualization: Yafei Nie, Petteri Uotila
Data curation: Yafei Nie, Xia Lin
Formal analysis: Yafei Nie, Qinghua Yang, Petteri Uotila
Funding acquisition: Qinghua Yang, Dake Chen
Investigation: Petteri Uotila
Methodology: Yafei Nie, Jiping Liu, Petteri Uotila
Software: Xia Lin
Supervision: Qinghua Yang, Dake Chen
Validation: Jiping Liu
Visualization: Yafei Nie, Xia Lin
Writing – original draft: Yafei Nie

Abstract Compared to the Coupled Model Intercomparison Project Phase 5 (CMIP5) climate models, the Antarctic sea ice area (SIA) has been improved in Phase 6 (CMIP6). However, the lack of knowledge about the reliability of sea ice dynamic and thermodynamic processes in the CMIP6 models still limits the accuracy of Antarctic sea ice projections. Here, by using a novel and systematic statistical metric, the performance of CMIP5 and CMIP6 models with near-realistic SIAs was assessed. We found improvements in CMIP6 models relative to CMIP5. Moreover, forcing the sea ice-ocean model with atmospheric reanalysis led to excessive ice convergence compared to the fully coupled ocean-sea ice-atmosphere model, although the SIA bias could be much smaller. This prevalent insufficient ice divergence in the models is highly correlated with the negative ice thickness bias, highlighting the importance of ice thickness in the correct simulation of sea ice dynamics.

Plain Language Summary Current state-of-the-art climate models do not reproduce the total area of Antarctic sea ice and its trends as observed. This impedes the use of climate models to understand changes in Antarctic sea ice over the past decades and to project its future. Separating how much of the simulated sea ice change is due to freezing and melting, and how much is due to ice transport allows us to identify physical causes for model biases, which helps us to optimize models. We examined the climate models that have simulated near-realistic sea ice areas between 1991 and 2009 and found significant improvements in their simulation of sea ice processes in the latest generation of models compared to the previous generation, although there is still much room for further improvement. As sea ice thickness and velocity interact, a key limitation of the state-of-the-art Antarctic sea ice simulation may stem from the general underestimation of ice thickness. This could be a critical issue to be targeted on the way toward increasingly skillful climate projections.

1. Introduction

Antarctic sea ice is a crucial component of the climate system. In contrast to the continued decline of Arctic sea ice, Antarctic sea ice extent (SIE) has experienced an overall increase from 1979 to 2015, followed by a subsequent dramatic decline and high interannual variability (Eayrs et al., 2021; Parkinson, 2019). In recent years, consecutive record summer minima (e.g., Liu et al., 2023; Parkinson & DiGirolamo, 2021; Raphael & Handcock, 2022; Turner et al., 2022) further complicate the puzzle of Antarctic sea ice change (Turner & Comiso, 2017).

One of the main challenges in explaining the Antarctic sea ice variability lies in the fact that the state-of-the-art climate models, such as Coupled Model Intercomparison Project Phase 5 (CMIP5) and Phase 6 (CMIP6) models, have large discrepancies and biases in simulating the historical sea ice mean states (Roach et al., 2020; Shu et al., 2020; Turner et al., 2013) and trends. The IPCC's sixth assessment report shows less confidence in Antarctic sea ice projections for the next few decades (Arias et al., 2021). These large model-observational mismatches prevent using climate models to confirm the hypotheses of mechanisms behind the Antarctic sea ice trends and variability (Blanchard-Wrigglesworth et al., 2021). Therefore, there is a need to diagnose and clarify the sources of biases in climate models and to provide detailed information on what to optimize in the next generation climate model sea-ice components.

Locally, sea ice evolves due to freezing, melting, transport, and deformation (Holland & Kwok, 2012). These processes synthesize air-ice-ocean interactions and have been reliably observed in the Southern Ocean (Holland & Kimura, 2016). This permits the Antarctic sea ice concentration (SIC) budget analysis. Over the last decade, the SIC budget diagnostics has become a tool to complement the traditional SIE and sea ice area (SIA) metrics

(Notz, 2014, 2015) when evaluating sea ice in climate models (e.g., Lecomte et al., 2016; Uotila et al., 2014), and in sea ice-ocean models (Nie et al., 2022, 2023). The SIC budget diagnostics have been used to attribute sea ice changes in the Southern Ocean to explain successive Antarctic summer SIE minima in recent years (Wang et al., 2022, 2023). To better understand the modeled sea ice physics, the CMIP6 Sea-Ice Model Intercomparison Project encouraged using sea ice budget diagnostics (Notz et al., 2016).

Holmes et al. (2019) comprehensively analyzed SIC budgets for CMIP5 models that simulated near-realistic SIAs and found that the ACCESS climate models reproduced the observed sea ice well. However, the CMIP6 SIC budgets have not yet been calculated and analyzed. Furthermore, in addition to the coupled climate model experiments, the Ocean Model Intercomparison Project (OMIP) experiments (Griffies et al., 2016) are included in the CMIP6 archive. The OMIP Phase 1 (OMIP1) and Phase 2 (OMIP2) experiments use the ice-ocean model exactly as in the historical CMIP experiments but are driven by Coordinated Ocean-ice Reference Experiments (CORE-II) forcing (Large & Yeager, 2009) and Japanese 55-year Reanalysis (JRA55-do) forcing (Tsujino et al., 2018), respectively.

Due to the reasons mentioned, we address the following research questions by evaluating the CMIP SIC budgets: (a) Is the Southern Ocean SIC budget in CMIP6 closer to observations compared to CMIP5? (b) What are the differences between the OMIP SIC budgets and the CMIP SIC budgets? What are the limitations of OMIP models? (c) What are the most beneficial directions to improve the sea ice simulation in the next generation of climate models?

2. Data and Methods

2.1. Data

Daily ice velocities obtained from the National Oceanic and Atmospheric Administration/National Snow and Ice Data Center (NOAA/NSIDC) Polar Pathfinder Daily 25 km EASE-Grid Version 4 product (Tschudi et al., 2019), and daily SICs obtained from the National Oceanic and Atmospheric Administration/National Snow and Ice Data Center (NOAA/NSIDC) Climate Data Record of Passive Microwave SIC, version 4 (CDR) (Meier et al., 2021) were used to calculate the observed SIC budget. Three daily SIC observational products were used to estimate the observational uncertainty (see Text S1 in Supporting Information S1). Due to the large snow thickness uncertainty, estimating the satellite-based sea ice thickness (SIT) is still a huge challenge. Here, SIT observations were derived from the Ice, Cloud and land Elevation Satellite (ICESat) by using an improved one-layer method (Xu et al., 2021), which has an uncertainty of 0.32 and 0.37 m in winter and spring, respectively.

Daily SIC based on CMIP5 historical experiments (RCP4.5 scenario experiments were used after 2006), CMIP6 historical experiments, and OMIP1 and OMIP2 experiments were used to calculate a monthly SIA climatology. In total, 24 CMIP5 and 22 CMIP6 models from 17 institutes, listed in Table S1 of Supporting Information S1, were included in this study, as they have both the daily SIC and the daily ice velocity available for the SIC budget diagnostics. Only the first ensemble member of each model was used for the analysis, as there are only minor SIC budget differences between the ensemble members of a single model (Holmes et al., 2019). The analysis was conducted for 1991–2009, dictated by the overlap between the OSI SAF ice velocity data (Text S1 in Supporting Information S1) and the OMIP1 output.

Monthly mean 10-m wind, sea level pressure (SLP), long-wave radiative flux, short-wave radiative flux, and sensible and latent heat fluxes from European Center for Medium-Range Weather Forecasts (ECMWF) Reanalysis (ERA5) (Hersbach et al., 2023), JRA55-do reanalysis and CORE-II reanalysis were used for the interpretation of the results.

The data used for calculating SIA were computed in the original grid of each data set. The other data, including model output and atmospheric reanalyses, were linearly interpolated to a 60 km polar stereographic grid using Climate Data Operator (CDO) (Schulzweida, 2022) version 2.0.4. In addition, the first-order conservative remapping method of CDO was used to interpolate from the unstructured grids of the AWI-CM-1-1-MR and AWI-ESM-1-1-LR CMIP6 models.

2.2. Sea Ice Concentration Budget

Following the ice mass conservation law, the SIC (expressed as A) budget equation for the integration in period t_1 to t_2 can be written as:

$$\int_{t_1}^{t_2} \frac{\partial A}{\partial t} dt = -\int_{t_1}^{t_2} \boldsymbol{u} \cdot \nabla A dt - \int_{t_1}^{t_2} A \nabla \cdot \boldsymbol{u} dt + \int_{t_1}^{t_2} (f - r) dt, \tag{1}$$

where $\boldsymbol{u}$ is the ice drift vector, f and r represent thermodynamic (freezing and melting) and redistribution (ridging and rafting) processes, respectively. Equation 1 decomposes the total local SIC change (denoted as dadt) into advection (first term on the right, denoted as adv), divergence (second term on the right, denoted as div) and the residual term (the rightmost term, denoted as res), which synthesizes the thermodynamic and redistribution processes. The calculation of the seasonal SIC budget follows the same approach as Holland and Kimura (2016) and the detailed calculation steps are given in Text S2 of Supporting Information S1.

2.3. Comprehensive Metrics for Evaluating Model Skills

We used the Distance between Indices of Simulation and Observation (DISO) metric (Hu et al., 2022) to evaluate the model performance. DISO is a newly proposed synthetic metric that combines multiple statistical metrics, thus reducing the risk of misleading conclusions. More details of the DISO metric can be found in Hu et al. (2019) and Zhou et al. (2021). In our study, it was calculated according to the following steps:

Step 1. For each model, compute four statistical metrics against the observations for each season and geographical sector surrounding Antarctica (Text S3 in Supporting Information S1). These metrics include: (a) mean absolute error (MAE), (b) root-mean-square error (RMSE), (c) correlation coefficient (CC), and (d) error of the area integral of SIC budget component as a proportion of the total SIC change (AIPE). The AIPE is defined as:

$$\mathrm{AIPE}_X = \frac{\int_{\sigma\in\Omega} X_M d\sigma}{\int_{\sigma\in\Omega} \mathrm{dadt}_M d\sigma} - \frac{\int_{\sigma\in\Omega} X_O d\sigma}{\int_{\sigma\in\Omega} \mathrm{dadt}_O d\sigma}, \tag{2}$$

where X represents ice budget component, Ω is the sectoral area of the Southern Ocean (south of 50°S). The subscripts M and O represent the model and observations, respectively. Thus, by definition, the $\mathrm{AIPE}_{\mathrm{dadt}}$ of the model is 0.

Step 2. Normalize the four metrics to be between 0 and 1, for example:

$$\mathrm{NMAE}_i = \frac{\mathrm{MAE}_i - \min(\mathrm{MAE})}{\max(\mathrm{MAE}) - \min(\mathrm{MAE})}, \tag{3}$$

where $i = 0,1,\cdots,m$, and m is the total number of models. The other three metrics were normalized accordingly and denoted as NRMSE, NCC, and NAIPE.

Step 3. Constructing the DISO metric based on the Euclidean distance of normalized sub-metrics obtained in the step 2:

$$\mathrm{DISO}_i = \sqrt{\mathrm{NMAE}_i^2 + \mathrm{NRMSE}_i^2 + (\mathrm{NCC}_i - 1)^2 + \left(\sqrt{\mathrm{NAIPE}_i}\right)^2}, \tag{4}$$

The NAIPE metric was squared to approximate a normal distribution and thus better differentiate the models (not shown).

Model-observed DISO metrics were separately calculated for each SIC budget component to obtain $\mathrm{DISO}_{\mathrm{dadt}}$, $\mathrm{DISO}_{\mathrm{adv}}$, $\mathrm{DISO}_{\mathrm{div}}$, and $\mathrm{DISO}_{\mathrm{res}}$ metrics for model intercomparison. Notably, these DISO metrics are comparable across the geographical sectors and between the seasons, but not between the DISO metrics (e.g., $\mathrm{DISO}_{\mathrm{dadt}}$ and $\mathrm{DISO}_{\mathrm{adv}}$).

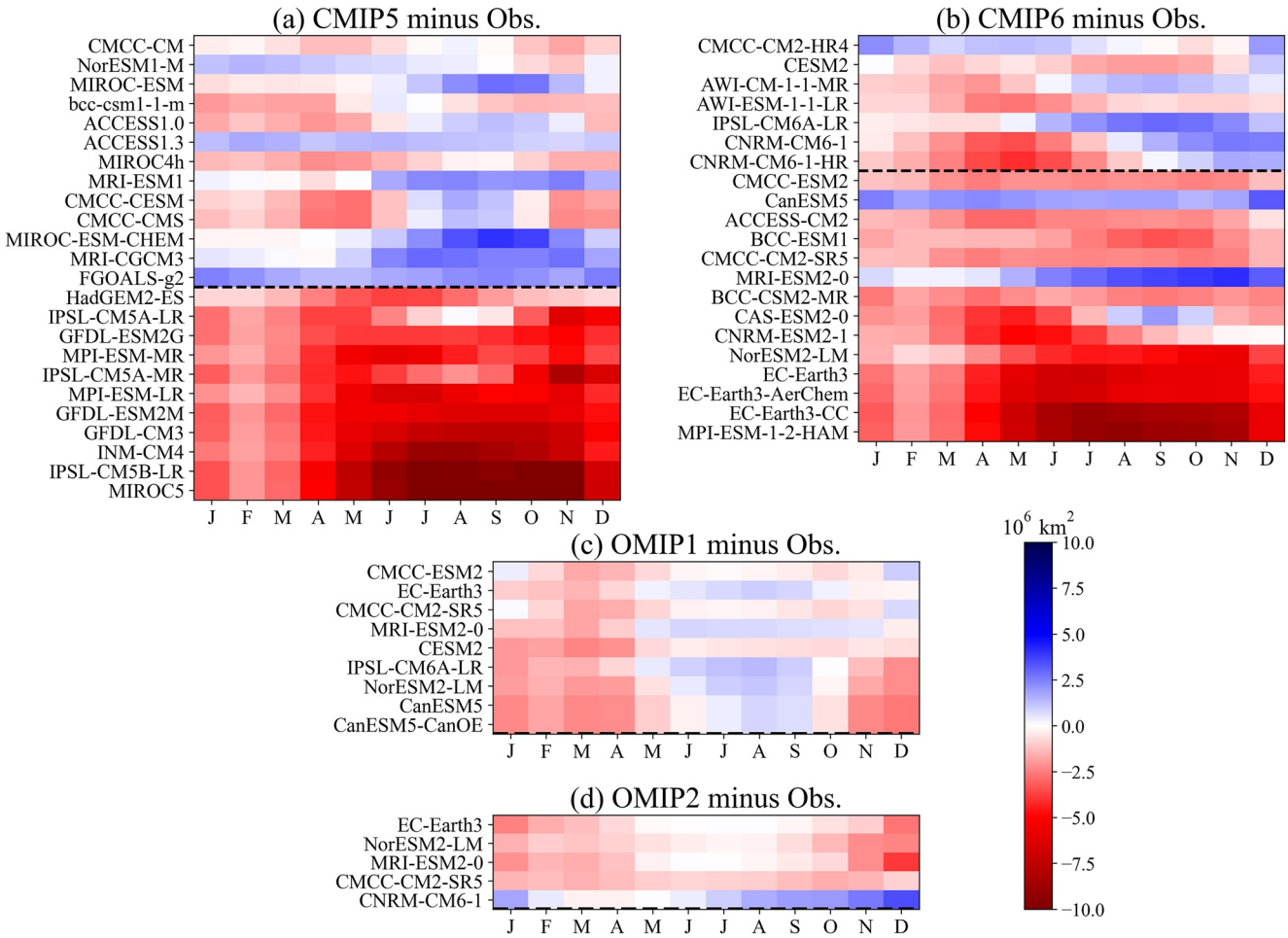

Figure 1. Monthly sea ice area differences between models and observations averaged from 1991 to 2009. Positive (blue) values indicate positive model biases. Models are ranked by the mean absolute error (MAE) of the 12 months; those above the black dashed line have an MAE less than $2 \times 10^6 km^2$ are considered to be in the best-performing model group.

3. Results and Discussions

3.1. Sea Ice Area

Figure 1 shows monthly climatological SIA differences between models and observations. The difference is set to 0 if it lies within the observational uncertainty (see Figure S1 in Supporting Information S1), but if a model overestimates (underestimates) SIA, the difference is from the upper (lower) bound of the observational uncertainty. Typically, climate models underestimate SIA (Roach et al., 2020). The OMIP models all reproduce near-realistic monthly SIA, OMIP2 usually being closer to observed than OMIP1. Following Holmes et al. (2019), a group of best-performing models with small monthly SIA biases was identified. This group included 13 CMIP5 models, 7 CMIP6 models, and all OMIP1 and OMIP2 models. These models were then selected for the following SIC budget analysis.

3.2. Sea Ice Concentration Budget Evaluation

The analysis focuses on the winter (June to August) and spring (September to November) SIC budgets due to the following reasons: (a) SIE in winter and spring is larger than in autumn (March to May), permitting a better comparison of performance across all sectors, (b) dynamic and thermodynamic sea ice processes are both important in winter and spring compared to summer (December to February) when the thermodynamics dominate, and (c) some other key sea ice variables, such as SIT, have more observations available in winter and spring.

The comparison of DISO metrics between CMIP5, CMIP6, OMIP1 and OMIP2 is illustrated in Figure 2. It can be seen that the average CMIP6 DISO is better (lower) than the CMIP5 one, for all SIC budget components and

10.1029/2023GL105265

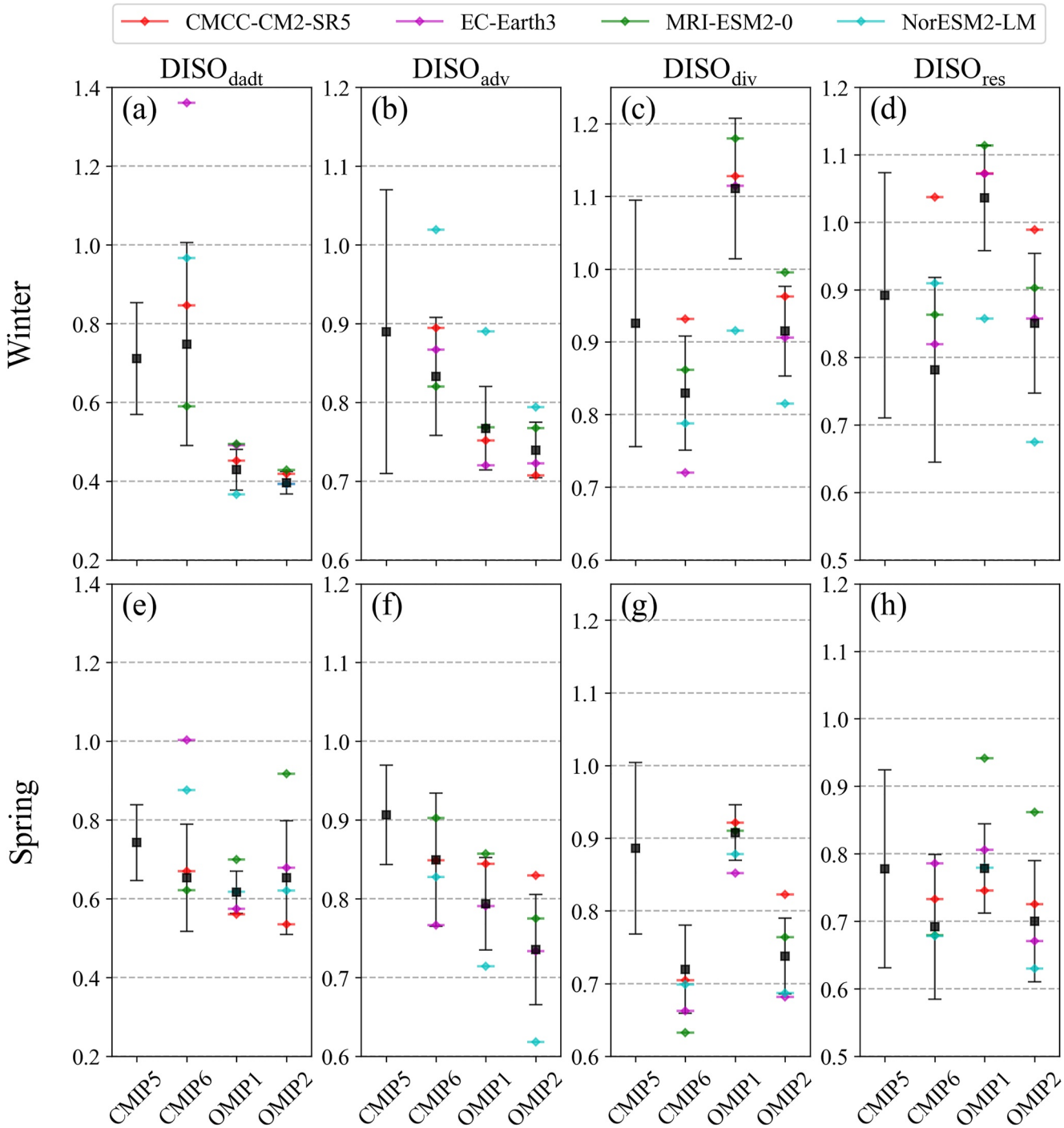

Figure 2. DISO metrics between the best performing models, as shown in Figure 1, and observations for each sea ice concentration budget component in (a–d) winter and (e–h) spring. Error bars denote one standard deviation. The four models that participated in all the CMIP6 historical, OMIP1 and OMIP2 experiments are marked with colored symbols. DISO is a dimensionless metric, with lower values indicating closer to observed data.

in both winter and spring. Also, the OMIP2 DISOs indicate improvements in sea ice processes from OMIP1. A further comparison of the four models that participated in both OMIP1 and OMIP2 (as marked in Figure 2) shows that the JRA55-do atmospheric forcing improves the sea ice dynamics (advection and divergence) and thermodynamics. This finding is consistent with Lin et al. (2023). It is worth noting that these results robustly hold for SIC budget comparisons against different observational data (see Text S4 and Figure S2 in Supporting Information S1), and Kimura et al. (2013) ice velocity observations in 2003–2009 would give comparable results (not

shown). Additionally, the better performance of CMIP6 compared to CMIP5, and OMIP2 compared to OMIP1 occurs in all geographical sectors (see Figure S3 in Supporting Information S1).

In addition, the DISO metrics of the four models that participated in both OMIP1 and OMIP2 highlight that the ice-ocean models driven by atmospheric reanalyses have more realistic sea ice advection than the fully coupled CMIP models. However, the OMIP sea ice divergence is not as realistic as in the CMIP models. Considering the assimilation of observations into atmospheric reanalyses, this result is somewhat surprising and possibly due to atmospheric reanalysis biases.

The best models in terms of average DISO metrics and per MIP are CMCC-CM (CMIP5), AWI-CM-1-1-MR (CMIP6), CESM2 (OMIP1) and NorESM2-LM (OMIP2). Of these, due to small RMSE and mean absolute error of dadt and adv, and higher CORRs of adv term, NorESM2-LM has the closest SIC budget compared to observations (Figures S4 and S5 in Supporting Information S1). AWI-CM-1-1-MR is the next one and has the most realistic $AIPE_{res}$, implying reasonable thermodynamics.

3.3. Comparison of CMIP6 Historical and OMIP Experiments

The previous section showed that the same CMIP6 model, when driven by prescribed atmospheric forcing (i.e., following the OMIP protocol), does not necessarily have a better SIA than its fully coupled version. Figure 3 presents the corresponding SIC budget differences of CMCC-CM2-SR5, allowing us to evaluate the model dynamics and thermodynamics performance separately.

The adv component is well reproduced and transports sea ice to the marginal ice zone as observed (Figures 3b1–b4). In the OMIP experiments, div is clearly unrealistic and dominated by convergence in contrast to the observations, which are dominated by divergence (Figure 3c1–c4). The JRA55-do results in a slightly better simulation compared to CORE-II. Related to the excessive convergence, the modeled res is also unrealistic (Figure 3d1–d4) negative values broadly occurring across the Southern Ocean, which in reality occur only in narrow Antarctic coastal zones (Holland & Kimura, 2016; Uotila et al., 2014). These characteristics are also present in other OMIP models (Figure S6 in Supporting Information S1).

The mean SLP, ice drift (Figure 3e1–e4), and heat flux (Figure 3f1–f4) were analyzed to elucidate the SIC budget results. It shows that the OMIP SLPs have the same spatial characteristics as the ERA5 SLP (Figure 3e). The CMIP historical SLP has a negative bias, but the locations of the low-pressure centers are in good agreement with ERA5. The modeled ice velocity is directed along the SLP isobars, which differs from the observed velocity that has a northward cross isobar component. This could be the direct cause of excessive convergence in the model, where the inner ice pack encounters too much compression and ridging. Without compression, sea ice drifts freely, and its northward velocity component correlates positively with the SIT (Leppäranta, 2011, chapter 6.1.1). Therefore, too thin SIT is the most plausible reason for the modeled ice drift direction along the isobars and the resulting excessive convergence (Figures 3g1–g4).

On the other hand, even though using JRA55-do instead of CORE-II slightly decreases the ice convergence and ridging, the inner ice pack growth in spring remains too small (Figure S7d3 and S7d4 in Supporting Information S1). This may be related to the surface heat flux bias in the model (Figure S7f3 and S7f4 in Supporting Information S1), inhibiting the sea ice formation in OMIP. In the CMIP historical experiments, the winter warm bias extends the sea ice melt to higher than observed latitudes, thus limiting their SIA (Figure 3f2).

Although the models have warm biases in winter and spring, their causes are different. The positive sensible and latent heat flux anomalies in winter mainly bring excess heat to the ice edge (Figure S8 in Supporting Information S1). In contrast, in spring, all surface heat flux components fluxes contribute to the excess warmth in the inner ice pack (Figure S9 in Supporting Information S1).

In summary, at least for the CMCC-CM2-SR5 model, JRA55-do results in a more realistic surface heat balance and SIA than CORE-II. However, due to its too thin SIT, its sea ice dynamics are not more realistic than its fully coupled version, despite the more reasonable atmospheric reanalysis-based SLP.

3.4. Connection Between Ice Thickness and Divergence

The relationship between SIT and divergence of the best-performing models is shown in Figure 4. As div always leads to dynamical sea ice decrease in both winter and spring, the area-integrated div contributes negatively/positively to the area-integrated dadt in winter/spring due to the overall formation/melting of sea ice, because dadt

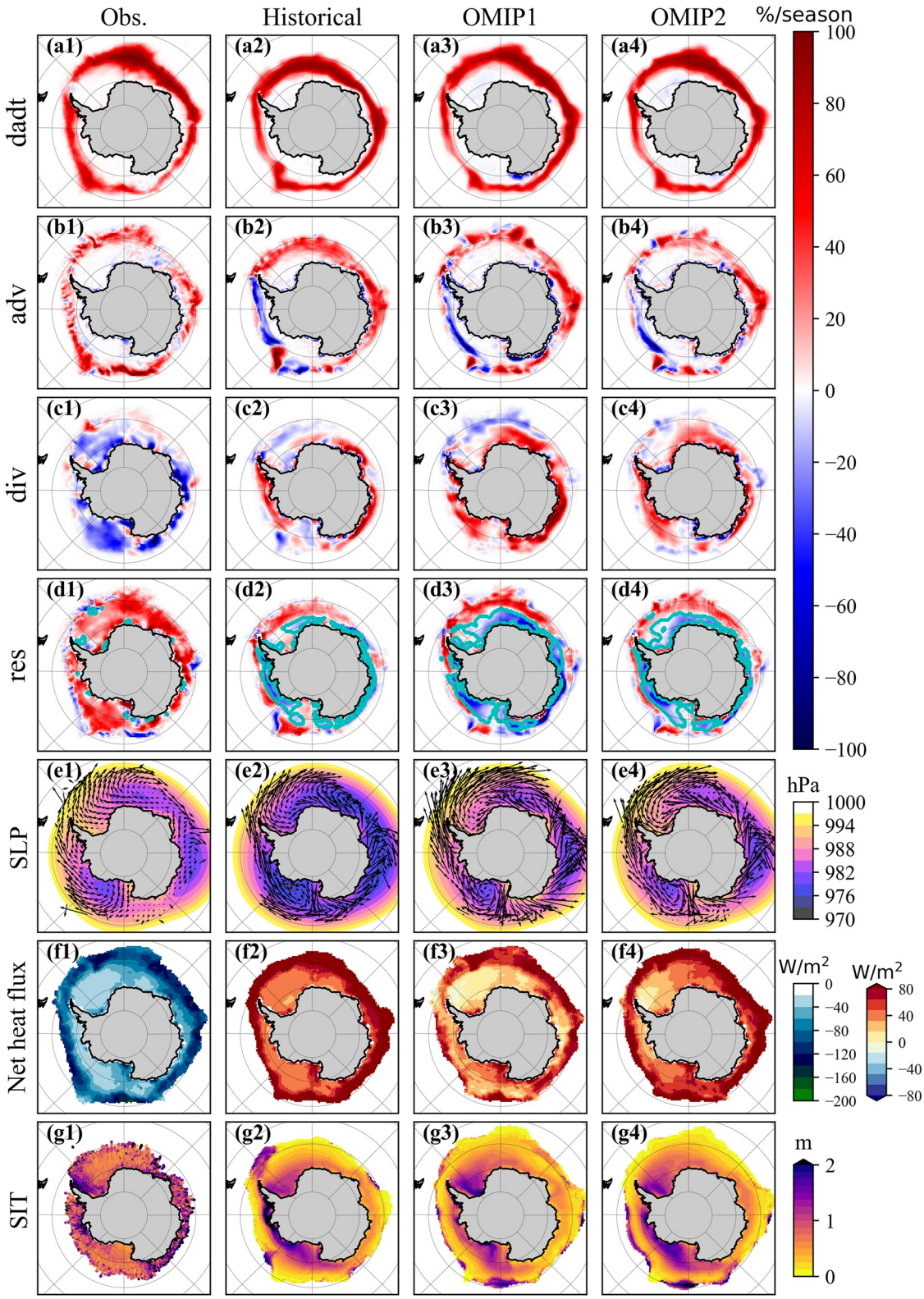

Figure 3. A comparison of the winter (the upper four rows) sea ice concentration budget components, (e1–e4) sea level pressure (SLP) overlaid with the ice drift vectors, (f1) net heat flux, (f2–f4) departures from (f1), and (g1–g4) sea ice thickness (SIT) of the (a1–g1) observations and the CMCC-CM2-SR5 (a2–g2) historical (a3–g3) OMIP1 and (a4–g4) OMIP2 experiments. All subplots are averaged over the winter of 1991–2009, except for (g1), the SIT averaged from May and June 2004–2006. (e1–e4) SLP from ERA5, historical experiment, CORE-II and JRA55-do. (f1) ERA5 net heat flux, (f2–f4) historical experiment, CORE-II and JRA55-do minus (f1). The net heat flux is negative when the surface loses heat to the atmosphere. The ridging areas are enclosed by cyan curves (d1–d4).

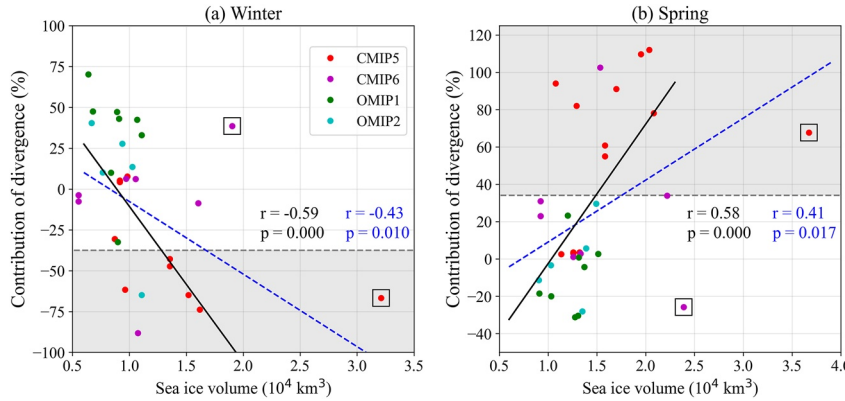

Figure 4. The area integral of div as a proportion of total sea ice change versus total sea ice volume for (a) winter and (b) spring. The blue dashed lines are linear regressions for all models, and the CCs and p-values are marked in blue. The solid black line is the regression after removing the two models with significantly unrealistic sea ice thickness patterns (marked by the black boxes). The gray horizontal line is the percentage contribution of the observed div, the models fall in the gray-filled region are overestimating sea ice divergence.

is positive in winter but negative in spring. Models having the opposite sign than the observed div have insufficient divergence (or excessive convergence), which usually relates to too thin sea ice (Figure 4). After excluding FGOALS-g2 in CMIP5 and CMCC-CM2-HR4 in CMIP6 with large positive SIT biases (SIT larger than 8 m in many regions) as outliers, the winter and spring correlation coefficients between sea ice volume and *div* become −0.59 and 0.58, respectively, with p-values less than 0.001. The corresponding correlations remain significant, with p-values less than 0.05, even when including the two outlying models.

Notably, the strong relationship between sea ice volume and *div* is consistent with Nie et al. (2022), who found that the Climate Forecast System Reanalysis (NCEP CFSR) had quite thick sea ice related to excessive divergence. Figure 4 results support their hypothesis of positive feedback between SIT and divergence.

4. Conclusions

The SIC budgets of CMIP5 and CMIP6 models with the most realistic SIAs were compared to the observational SIC budget using a comprehensive statistical metric. The results revealed encouraging improvements in all CMIP6 SIC budget components compared to CMIP5, although some limitations remain; for example, the inner pack ice divergence and formation in spring are deficient. The JRA55-do atmospheric forcing reduces the air-sea sensible heat flux compared to the fully coupled model, which greatly improves the SIA simulations, but also results in excessive sea ice convergence. This is related to too thin modeled sea ice leading to too slow northward drift, hindering the sea ice transport to lower latitudes. Excessive convergence also promotes ridging. In the best-performing CMIP5, CMIP6, OMIP1, and OMIP2 models, the correlation between the convergence (or analogously divergence) and SIT was high.

A positive feedback mechanism may exist between SIT and divergence. Negative SIT biases result in insufficient divergence, which in turn inhibits the formation of open water in the inner ice pack and new ice formation in winter. This reduced ice formation limits the sea ice volume, including the average SIT. As this feedback mechanism can amplify sea ice velocity and thickness biases, the improvement of modeled SIT and ice drift is emphasized. For example, Sun and Eisenman (2021) simulated the Antarctic SIE expansion during 1979–2015 consistent with the observations by replacing the modeled sea ice velocities with observed ones.

Accurately evaluating the SIC budget in the climate models is crucial for at least two reasons. First, comparing the SIC budget components with observations can determine the relative contributions of dynamics and thermodynamics on model biases (e.g., Uotila et al., 2014). Second, freezing, melting, and sea ice transport plays a crucial role in regulating the freshwater transport and salinity distribution in the Southern Ocean, thus profoundly influencing the global ocean circulation and ice sheet melt (e.g., Abernathey et al., 2016; Haumann et al., 2016). The progress from CMIP5 to CMIP6 regarding sea ice is encouraging, yet the feedback between SIT and divergence requires further research.

Conflict of Interest

The authors declare no conflicts of interest relevant to this study.

Data Availability Statement

All data used in the study are open-access. The Polar Pathfinder ice drift and CDR ice concentration data are available at Tschudi et al. (2019) and Meier et al. (2021). CMIP data can be downloaded from the ESGF data portals (see https://esgf-node.llnl.gov/search/cmip5/ and https://esgf-node.llnl.gov/search/cmip6). The CMIP5 and CMIP6 models used can be found in Table S1 of Supporting Information S1. The ERA5 reanalysis is available at Hersbach et al. (2023). The JRA55-do reanalysis can be accessed from Tsujino et al. (2019). The SIT data derived from the ICESat is available at Xu et al. (2020). The OSI SAF SIC data can be downloaded from Copernicus Marine Service (2017). The OSI-455 ice drift observations are available at OSI SAF (2022).

Acknowledgments
This study was funded by the National Key R&D Program of China (No. 2022YFE0106300), the National Natural Science Foundation of China (No. 41941009), and the Southern Marine Science and Engineering Guangdong Laboratory (Zhuhai) (No. SML2022SP401). This study contributes to the Year of Polar Prediction, a flagship activity of the Polar Prediction Project, initiated by the World Weather Research Programme of the World Meteorological Organization. Petteri Uotila was supported by the Academy of Finland (project 322432) and the European Union's Horizon 2020 research and innovation framework programme (PolarRES project, Grant 101003590).

References

Abernathey, R. P., Cerovecki, I., Holland, P. R., Newsom, E., Mazloff, M., & Talley, L. D. (2016). Water-mass transformation by sea ice in the upper branch of the Southern Ocean overturning. *Nature Geoscience*, *9*(8), 596–601. https://doi.org/10.1038/ngeo2749

Arias, P. A., Bellouin, N., Jones, R. G., Naik, V., Plattner, G.-K., Rogelj, J., et al. (2021). Technical Summary. In *Climate Change 2021: The Physical Science Basis. Contribution of Working Group I to the Sixth Assessment Report of the Intergovernmental Panel on Climate Change*. https://doi.org/10.1017/9781009157896.002

Blanchard-Wrigglesworth, E., Roach, L. A., Donohoe, A., & Ding, Q. (2021). Impact of winds and Southern Ocean SSTs on Antarctic sea ice trends and variability. *Journal of Climate*, *34*(3), 949–965. https://doi.org/10.1175/JCLI-D-20-0386.1

Copernicus Marine Service. (2017). Global Ocean Sea Ice Concentration Time Series REPROCESSED (OSI-SAF) [Dataset]. Copernicus Marine Service. https://doi.org/10.48670/moi-00136

Eayrs, C., Li, X., Raphael, M. N., & Holland, D. M. (2021). Rapid decline in Antarctic sea ice in recent years hints at future change. *Nature Geoscience*, *14*(7), 460–464. https://doi.org/10.1038/s41561-021-00768-3

Griffies, S. M., Danabasoglu, G., Durack, P. J., Adcroft, A. J., Balaji, V., Böning, C. W., et al. (2016). OMIP contribution to CMIP6: Experimental and diagnostic protocol for the physical component of the Ocean Model Intercomparison Project. *Geoscientific Model Development*, *9*(9), 3231–3296. https://doi.org/10.5194/gmd-9-3231-2016

Haumann, F. A., Gruber, N., Münnich, M., Frenger, I., & Kern, S. (2016). Sea-ice transport driving Southern Ocean salinity and its recent trends. *Nature*, *537*(7618), 89–92. https://doi.org/10.1038/nature19101

Hersbach, H., Bell, B., Berrisford, P., Biavati, G., Horányi, A., Muñoz Sabater, J., et al. (2023). *ERA5 monthly averaged data on single levels from 1940 to present*. Copernicus Climate Change Service (C3S) Climate Data Store (CDS). https://doi.org/10.24381/cds.f17050d7

Holland, P. R., & Kimura, N. (2016). Observed concentration budgets of Arctic and Antarctic sea ice. *Journal of Climate*, *29*(14), 5241–5249. https://doi.org/10.1175/JCLI-D-16-0121.1

Holland, P. R., & Kwok, R. (2012). Wind-driven trends in Antarctic sea-ice drift. *Nature Geoscience*, *5*(12), 872–875. https://doi.org/10.1038/ngeo1627

Holmes, C. R., Holland, P. R., & Bracegirdle, T. J. (2019). Compensating biases and a noteworthy success in the CMIP5 representation of Antarctic sea ice processes. *Geophysical Research Letters*, *46*(8), 4299–4307. https://doi.org/10.1029/2018GL081796

Hu, Z., Chen, D., Chen, X., Zhou, Q., Peng, Y., Li, J., & Sang, Y. (2022). CCHZ-DISO: A timely new assessment system for data quality or model performance from Da Dao Zhi Jian. *Geophysical Research Letters*, *49*(23), e2022GL100681. https://doi.org/10.1029/2022GL100681

Hu, Z., Chen, X., Zhou, Q., Chen, D., & Li, J. (2019). DISO: A rethink of Taylor diagram. *International Journal of Climatology*, *39*(5), 2825–2832. https://doi.org/10.1002/joc.5972

Kimura, N., Nishimura, A., Tanaka, Y., & Yamaguchi, H. (2013). Influence of winter sea-ice motion on summer ice cover in the Arctic. *Polar Research*, *32*(1), 20193. https://doi.org/10.3402/polar.v32i0.20193

Large, W. G., & Yeager, S. G. (2009). The global climatology of an interannually varying air–sea flux data set. *Climate Dynamics*, *33*(2–3), 341–364. https://doi.org/10.1007/s00382-008-0441-3

Lecomte, O., Goosse, H., Fichefet, T., Holland, P. R., Uotila, P., Zunz, V., & Kimura, N. (2016). Impact of surface wind biases on the Antarctic sea ice concentration budget in climate models. *Ocean Modelling*, *105*, 60–70. https://doi.org/10.1016/j.ocemod.2016.08.001

Leppäranta, M. (2011). *The drift of sea ice* (2nd ed.). Springer.

Lin, X., Massonnet, F., Fichefet, T., & Vancoppenolle, M. (2023). Impact of atmospheric forcing uncertainties on Arctic and Antarctic sea ice simulations in CMIP6 OMIP models. *The Cryosphere*, *17*(5), 1935–1965. https://doi.org/10.5194/tc-17-1935-2023

Liu, J., Zhu, Z., & Chen, D. (2023). Lowest Antarctic sea ice record broken for the second year in a row. *Ocean-Land-Atmosphere Research*, *2*, 0007. https://doi.org/10.34133/olar.0007

Meier, W. N., Fetterer, F., Windnagel, A. K., & Stewart, J. S. (2021). NOAA/NSIDC Climate Data Record of Passive Microwave Sea Ice Concentration, Version 4 [Dataset]. NASA National Snow and Ice Data Center Distributed Active Archive Center. https://doi.org/10.7265/efmz-2t65

Nie, Y., Li, C., Vancoppenolle, M., Cheng, B., Boeira Dias, F., Lv, X., & Uotila, P. (2023). Sensitivity of NEMO4.0-SI^3 model parameters on sea ice budgets in the Southern Ocean. *Geoscientific Model Development*, *16*(4), 1395–1425. https://doi.org/10.5194/gmd-16-1395-2023

Nie, Y., Uotila, P., Cheng, B., Massonnet, F., Kimura, N., Cipollone, A., & Lv, X. (2022). Southern Ocean sea ice concentration budgets of five ocean-sea ice reanalyses. *Climate Dynamics*, *59*(11–12), 3265–3285. https://doi.org/10.1007/s00382-022-06260-x

Notz, D. (2014). Sea-ice extent and its trend provide limited metrics of model performance. *The Cryosphere*, *8*(1), 229–243. https://doi.org/10.5194/tc-8-229-2014

Notz, D. (2015). How well must climate models agree with observations? *Philosophical Transactions of the Royal Society A: Mathematical, Physical & Engineering Sciences*, *373*(2052), 20140164. https://doi.org/10.1098/rsta.2014.0164

Notz, D., Jahn, A., Holland, M., Hunke, E., Massonnet, F., Stroeve, J., et al. (2016). The CMIP6 Sea-Ice Model Intercomparison Project (SIMIP): Understanding sea ice through climate-model simulations. *Geoscientific Model Development*, *9*(9), 3427–3446. https://doi.org/10.5194/gmd-9-3427-2016

OSI SAF. (2022). Global Sea Ice Drift Climate Data Record Release v1.0 - Multimission. *EUMETSAT SAF on Ocean and Sea Ice*. https://doi.org/10.15770/EUM_SAF_OSI_0012

Parkinson, C. L. (2019). A 40-y record reveals gradual Antarctic sea ice increases followed by decreases at rates far exceeding the rates seen in the Arctic. *Proceedings of the National Academy of Sciences*, *116*(29), 14414–14423. https://doi.org/10.1073/pnas.1906556116

Parkinson, C. L., & DiGirolamo, N. E. (2021). Sea ice extents continue to set new records: Arctic, Antarctic, and global results. *Remote Sensing of Environment*, *267*, 112753. https://doi.org/10.1016/j.rse.2021.112753

Raphael, M. N., & Handcock, M. S. (2022). A new record minimum for Antarctic sea ice. *Nature Reviews Earth & Environment*, *3*(4), 215–216. https://doi.org/10.1038/s43017-022-00281-0

Roach, L. A., Dörr, J., Holmes, C. R., Massonnet, F., Blockley, E. W., Notz, D., et al. (2020). Antarctic sea ice area in CMIP6. *Geophysical Research Letters*, *47*(9), e2019GL086729. https://doi.org/10.1029/2019GL086729

Schulzweida, U. (2022). CDO user guide (version 2.1.0) [Software]. Zenodo. https://doi.org/10.5281/zenodo.7112925

Shu, Q., Wang, Q., Song, Z., Qiao, F., Zhao, J., Chu, M., & Li, X. (2020). Assessment of sea ice extent in CMIP6 with comparison to observations and CMIP5. *Geophysical Research Letters*, *47*(9), e2020GL087965. https://doi.org/10.1029/2020GL087965

Sun, S., & Eisenman, I. (2021). Observed Antarctic sea ice expansion reproduced in a climate model after correcting biases in sea ice drift velocity. *Nature Communications*, *12*(1), 1060. https://doi.org/10.1038/s41467-021-21412-z

Tschudi, M. A., Meier, W. N., Stewart, J. S., Fowler, C., & Maslanik, J. (2019). Polar Pathfinder Daily 25 km EASE-Grid Sea Ice Motion Vectors, Version 4 [Dataset]. NASA National Snow and Ice Data Center Distributed Active Archive Center. https://doi.org/10.5067/INAWUWO7QH7B

Tsujino, H., Urakawa, S., Nakano, H., Small, R. J., Kim, W. M., Yeager, S. G., et al. (2018). JRA-55 based surface dataset for driving ocean–sea-ice models (JRA55-do). *Ocean Modelling*, *130*, 79–139. https://doi.org/10.1016/j.ocemod.2018.07.002

Tsujino, H., Urakawa, S., Nakano, H., Small, R. J., Kim, W. M., Yeager, S. G., et al. (2019). input4MIPs.CMIP6.OMIP.MRI.MRI-JRA55-do-1-4-0 [Dataset]. Earth System Grid Federation. https://doi.org/10.22033/ESGF/input4MIPs.10842

Turner, J., Bracegirdle, T. J., Phillips, T., Marshall, G. J., & Hosking, J. S. (2013). An initial assessment of Antarctic sea ice extent in the CMIP5 models. *Journal of Climate*, *26*(5), 1473–1484. https://doi.org/10.1175/JCLI-D-12-00068.1

Turner, J., & Comiso, J. (2017). Solve Antarctica's sea-ice puzzle. *Nature*, *547*(7663), 275–277. https://doi.org/10.1038/547275a

Turner, J., Holmes, C., Caton Harrison, T., Phillips, T., Jena, B., Reeves-Francois, T., et al. (2022). Record low Antarctic sea ice cover in February 2022. *Geophysical Research Letters*, *49*(12), e2022GL098904. https://doi.org/10.1029/2022GL098904

Uotila, P., Holland, P. R., Vihma, T., Marsland, S. J., & Kimura, N. (2014). Is realistic Antarctic sea-ice extent in climate models the result of excessive ice drift? *Ocean Modelling*, *79*, 33–42. https://doi.org/10.1016/j.ocemod.2014.04.004

Wang, J., Luo, H., Yang, Q., Liu, J., Yu, L., Shi, Q., & Han, B. (2022). An unprecedented record low Antarctic sea-ice extent during austral summer 2022. *Advances in Atmospheric Sciences*, *39*(10), 1591–1597. https://doi.org/10.1007/s00376-022-2087-1

Wang, J., Luo, H., Yu, L., Li, X., Holland, P. R., & Yang, Q. (2023). The impacts of combined SAM and ENSO on seasonal Antarctic sea ice changes. *Journal of Climate*, *36*(11), 3553–3569. https://doi.org/10.1175/JCLI-D-22-0679.1

Xu, Y., Li, H., Liu, B., Xie, H., & Ozsoy-Cicek, B. (2020). Antarctic Sea-Ice Thickness and Volume from NASA's ICESat/ICESat-2 Missions [Dataset]. Figshare. https://doi.org/10.6084/m9.figshare.12910121.v4

Xu, Y., Li, H., Liu, B., Xie, H., & Ozsoy-Cicek, B. (2021). Deriving Antarctic Sea-Ice Thickness from Satellite Altimetry and estimating Consistency for NASA's ICESat/ICESat-2 Missions. *Geophysical Research Letters*, *48*(20). https://doi.org/10.1029/2021GL093425

Zhou, Q., Chen, D., Hu, Z., & Chen, X. (2021). Decompositions of Taylor diagram and DISO performance criteria. *International Journal of Climatology*, *41*(12), 5726–5732. https://doi.org/10.1002/joc.7149